Plasmon responses and optical chirality of helical nanoparticle assemblies

ARTICLE · FEBRUARY 2012

2 AUTHORS, INCLUDING:

Zhiyuan Fan
Ohio University
28 PUBLICATIONS **1,256** CITATIONS

SEE PROFILE

NANO LETTERS

pubs.acs.org/NanoLett

Plasmonic Circular Dichroism of Chiral Metal Nanoparticle Assemblies

Zhiyuan Fan, and Alexander O. Govorov*

Department of Physics and Astronomy, Ohio University, Athens, Ohio 45701

ABSTRACT We describe from the theoretical point of view a plasmonic mechanism of optical activity in chiral complexes composed of metal nanoparticles (NPs). In our model, the circular dichroism (CD) signal comes from the Coulomb interaction between NPs. We show that the CD spectrum is very sensitive to the geometry and composition of a chiral complex and also has typically both positive and negative bands. In our calculations, the strongest CD signals were found for the helix geometry resembling helical structures of many biomolecules. For chiral tetramers and pyramids, the symmetry of a frame of a complex is very important for the formation of a strong CD response. Chiral natural molecules (peptides, DNA, etc.) often have strong CD signals in the UV range and typically show weak CD responses in the visible range of photon energies. In contrast to the natural molecules, the described mechanism of plasmonic CD is able to create strong CD signals in the visible wavelength range. This plasmonic mechanism offers a unique possibility to design colloidal and other nanostructures with strong optical chirality.

KEYWORDS Nanoparticles, optical properties, circular dichroism, plasmons

Optical circular dichroism (CD) spectroscopy reveals chiral properties of molecules and biomolecules.[1] A molecular object is chiral and exhibits an optical CD effect if it has neither mirror-symmetry planes nor a center of symmetry. In this case, a molecule acquires a sense of rotation (clockwise or counterclockwise) and hence it reacts on right- and left-handed photons differently and therefore shows a nonzero CD signal. The CD measurement is one of the most important methods in the spectroscopy of biomolecules.[1] This method allows us to observe conformational changes of complex biomolecules such as peptides, proteins, DNA, and so forth. Importantly, strong CD signals from chiral molecules and biomolecules are typically found in the UV range (~200−300 nm) whereas a CD strength of molecules in the visible range is weak. Often strong CD signals in the UV range come from the helical geometry of molecular and biomolecular systems. In this paper, we show that, using artificial chiral optically active nanoparticle complexes, one can create a strong CD effect in the visible range. Nanostructures with strong optical chirality in the visible range can potentially be used for biosensors and for optoelectronic devices. In particular, such nanostructures can potentially be employed as chiral nanoscale elements to create negative refractive index materials.[2]

One important topic in the modern nanotechnology concerns assembly and optical studies of complexes comprising metal NPs, semiconductor quantum dots, and biomolecules.[3−8] Coulomb and electromagnetic interactions between nanocrystals in such complexes are very prominent and often govern their optical responses.[9−14] In particular, interactions between metal NPs can be very strong due to strong plasmonic fields.[5,15−19] One way to fabricate NP complexes composed of few metal NPs is to use biolinkers. Such Au-NP complexes, assembled using DNAs and peptides, have been already realized.[20−22] We think however that even better control of geometry of a complex can be achieved using rigid DNA origami frames[23] with biolinkers. In this paper, we describe and numerically calculate the CD effect originating from plasmonic interactions between metal NPs. We show that the geometry and precise positioning of NPs are very important. Adding or removing one NP can change a CD spectrum dramatically. This effect is especially prominent in the helical NP complexes. Since a plasmonic CD spectrum has both positive and negative bands, a high degree of homogeneity in a macroscopic ensemble of complexes in a solution is needed to achieve a strong CD signal.

So far, most of the optical studies on chiral nanocrystals concern semiconductor and metal NPs with a chiral molecular adsorbate.[24−27] In such systems, CD responses of NPs are associated with adsorbed chiral molecules.[28] Other mechanisms of new CD responses originate from the plasmon enhancement of chiral molecules[29] and from the interaction between a chiral molecular dipole and a metal NP.[30] This paper studies a qualitatively different CD mechanism coming from plasmonic interactions between NPs in a chiral complex. Similar plasmonic mechanism of CD was suggested in the experimental paper.[21] Indeed, the paper[21] reported CD signals at the Au-plasmon wavelength in NP assemblies. However, exact identification of the CD mechanism in ref 21 is challenging since the system (NP solution) in the paper[21] included NP complexes of various geometries and compositions and, in addition, these NP complexes incorporated chiral DNA linkers. Another relevant research

* To whom correspondence should be addressed. E-mail: Govorov@ohiou.edu.
Received for review: 04/8/2010
Published on Web: 06/10/2010

DOI: 10.1021/nl101231b | *Nano Lett.* **2010,** *10,* 2580–2587

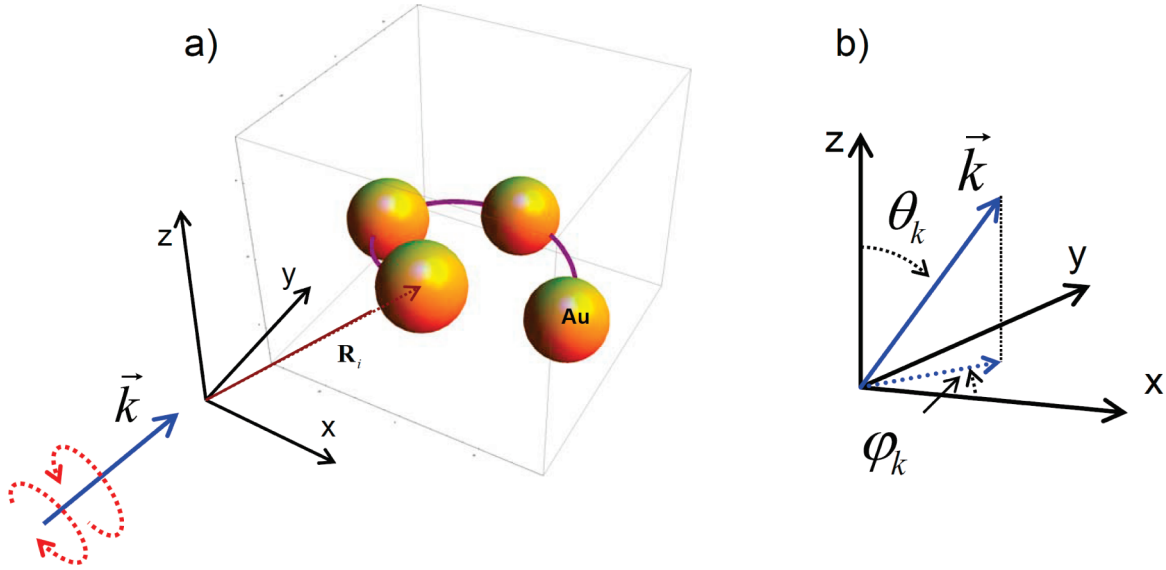

FIGURE 1. (a) Schematics of a complex composed of metal nanoparticles coupled by Coulomb and electromagnetic interactions; $\vec{R}_i$ is the position vector of *i*-NP. (b) System of coordinates and the definition of polar angles for the photon wavevector used in the text.

direction concerns optical activity in random and nanostructure films. In a film with random metal NP aggregates, near-field optical spectra revealed local optical handedness which had a mesoscopic character.[31] A film with a two-dimensional "chiral" metal pattern exhibited a controllable effect of polarization rotation.[32]

We also should comment that the physical mechanism, calculated in this paper, has some similarity with the optical chirality due to the Coulomb dipole−dipole interaction in a large chiral molecule (e.g., in the α-helix or DNA).[1] However, there are very important differences between the plasmonic CD described here and the CD effect in biomolecules: (1) The mechanism of optical responses in our system is plasmonic, whereas optical responses of biomolecules come from excitons. (2) The plasmonic CD can appear in the visible range, whereas molecular CD signals are mostly in the UV range. (3) A complex biomolecule is composed of interacting chromophores (elementary blocks) and each chromophore is described as a single dipole. In NPs complexes, an elementary block (NP) has three plasmonic dipoles.

Formalism. We now consider a complex composed of metal NPs interacting via the dipolar Coulomb and electromagnetic interactions. The complex experiences the field of an incident electromagnetic wave: $\vec{E}_{\text{external}} = \text{Re}[\vec{E}_{\text{ext},\omega} \cdot e^{-i\omega t}]$, where $\vec{E}_{\text{ext},\omega} = \vec{e}_0 E_0 e^{i\vec{k}\varepsilon_0^{1/2}\vec{r}}$ and $\vec{e}_0$ is the polarization vector, $k = 2\pi/\lambda_0$, and λ_0 is the wavelength of light in vacuum. The energy flux of the incident wave is given by $I_0 = [E_0^2 c_0 \sqrt{\varepsilon_0}]/8\pi$, where ε_0 is the dielectric constant of the matrix. In the following, we will take water as a matrix material ($\varepsilon_0 = 1.8$). The radii of NPs are denoted by a_i, where i is the NP number. The position vectors of NPs are $\vec{r}_i$ and $\vec{r}_{ij} = \vec{r}_j - \vec{r}_i$. Then, the unit vector pointing from i-NP to j-NP $\vec{n}_{ij} = \vec{n}_{i\to j} = (\vec{r}_j - \vec{r}_i)/r_{ij}$.

A circularly polarized electromagnetic wave approaches the system at arbitrary polar angles θ_k and φ_k (Figure 1b). The CD signal is defined as a difference between two absorptions

$$\text{CD} = \langle Q_+ - Q_- \rangle_\Omega \tag{1}$$

where the averaging over the solid angle, $\langle ... \rangle_\Omega$, is needed since complexes are in a solution and have random orientations. $Q_{+(-)}$ are the rates of absorption for two incident electromagnetic waves with the polarization

$$\vec{e}_{0\pm} = \frac{\vec{e}_\theta \pm i\vec{e}_\phi}{\sqrt{2}} \tag{2}$$

where $\vec{e}_{\theta(\phi)}$ are the orthogonal unit vectors along the directions perpendicular to the wave vector; $\vec{e}_{\theta(\phi)} \perp \vec{k}$ and the vector $\vec{e}_\phi$ lies in the $x-y$ plane. The averaging in eq 1 can be done in two ways. (1) A NP complex is rotated, whereas the incident angles of the electromagnetic wave (θ_k and φ_k) are kept constant. (2) The internal axes of the complex are fixed and the electromagnetic waves with polarizations ± approach the complex from all possible directions. These ways to perform the averaging are equivalent.[33] In experiments with a solution, NP complexes have random orientations but the wavevector of incident light ($\vec{k}$) has a well-defined direction. Therefore, in a solution, one should perform averaging over all possible orientations of the complex. But, here we will use the method 2 since it is more convenient. In other words, we will perform averaging over all directions of $\vec{k}$.

The absorption rates of plasmonic NPs for the two incident waves (±) are calculated as $Q_\pm = (1/2)\text{Re}\int_V \vec{J}^*_{\omega,\pm}(\vec{r}) \cdot \vec{E}_{\omega,\pm}(\vec{r})\, dV$, where $\vec{J}^*_{\omega,\pm}$ and $\vec{E}_{\omega,\pm}$ are the complex amplitudes of the indu-

DOI: 10.1021/nl101231b | *Nano Lett.* **2010,** *10,* 2580–2587

ced electric current and total electric field, respectively; the actual current and field are then given by $\vec{j}(r) = \mathrm{Re}\,[\vec{j}_{\omega,\pm}(r)\cdot e^{-i\omega t}]$ and $\vec{E}(\vec{r}) = \mathrm{Re}[\vec{E}_{\omega,\pm}(\vec{r})\cdot e^{-i\omega t}]$, respectively. In the dipole approximation, the electric dipole of a single NP is given by

$$\vec{d}_i = \alpha_i \cdot \vec{E}_{\mathrm{tot},\omega,i} = \alpha_i \cdot (\vec{E}_{\mathrm{ext},\omega,i} + \vec{E}_{\mathrm{induced},\omega,i})$$

where $\vec{E}_{\mathrm{tot},\omega,i} = \vec{E}_{\mathrm{ext},\omega,i} + \vec{E}_{\mathrm{induced},\omega,i}$ is the field acting on the i-NP; $\vec{E}_{\mathrm{ext},\omega,i} = \vec{E}_{\mathrm{ext},\omega}(\vec{r}_i)$ and $\vec{E}_{\mathrm{induced},\omega,i}$ is the field induced by all other NPs with $j \neq i$. Considering a pointlike dipole, we obtain[34]

$$\vec{E}_{\mathrm{induced},\omega,i} = \sum_{j\neq i}\left[\frac{3(\vec{d}_j\cdot\vec{n}_{ji})\cdot\vec{n}_{ji} - \vec{d}_j}{\varepsilon_0\cdot r_{ij}^3}(1 - ik\sqrt{\varepsilon_0}r_{ij}) + \frac{\omega^2}{c_0^2}\frac{\vec{d}_j - (\vec{d}_j\cdot\vec{n}_{ji})\cdot\vec{n}_{ji}}{r_{ij}}\right]e^{ik\sqrt{\varepsilon_0}r_{ij}} \quad (3)$$

where $\alpha_i(\omega) = a_i^3[(\varepsilon_{\mathrm{NP},i} - \varepsilon_0)/(\varepsilon_{\mathrm{NP},i} + 2\varepsilon_0)]$ is the i-NP polarizability, $\varepsilon_{\mathrm{NP},i} = \varepsilon_{\mathrm{NP},i}(\omega)$ is the metal dielectric function, and $\bar{c} = c_0/(\varepsilon_0)^{1/2}$ is the light speed in the medium (water). Then, one can show that the total absorption cross section can be calculated as

$$\sigma_\pm = \frac{Q_\pm}{I_0} = \varepsilon_0\frac{8\pi}{2\cdot E_0^2\cdot c_0\sqrt{\varepsilon_0}}\omega\mathrm{Im}\left[\sum_i\frac{\vec{d}_{i,\pm}^{\,*}\cdot\vec{d}_{i,\pm}}{\alpha_i^*(\omega)}\right] \quad (4)$$

which has the units on cm^2. The dipoles $\vec{d}_{i,\pm}$ are related to the incident electromagnetic waves $\pm$. In the absence of internal retardation effects ($k\rightarrow 0$ in eq 3), the cross section can be reduced to

$$\sigma_\pm = \varepsilon_0\frac{8\pi}{2\cdot E_0^2\cdot c_0\sqrt{\varepsilon_0}}\omega\mathrm{Im}\left[\left(\sum_i E^*_{\mathrm{external},\omega,i,\pm}\cdot\vec{d}_{i,\pm}\right)\right] \quad (5)$$

The molar extinction and the molar CD in the convenient units of cm$^{-1}\cdot$M^{-1} are written as

$$\varepsilon_\pm = \left(\frac{N_A}{0.23}\right)10^4\varepsilon_0\frac{8\pi}{2\cdot E_0^2\cdot c_0\sqrt{\varepsilon_0}}\omega\mathrm{Im}\left[\sum_i\frac{\vec{d}_{i,\pm}^{\,*}\cdot\vec{d}_{i,\pm}}{\alpha_i^*(\omega)}\right]$$
$$\varepsilon_{CD} = \langle\varepsilon_+ - \varepsilon_-\rangle_\Omega \quad (6)$$

In the following, we will use eqs 6 a lot in our calculations. Since the electric dipoles $\vec{d}_i$ interact, we have to solve the self-consistent problem. With help of eq 3, the system of equations $\vec{d}_i = \alpha_i\cdot\vec{E}_{tot,\omega,i}$ can be written as

$$\vec{d}_i = \alpha_i\left(\vec{E}_{\mathrm{ext},\omega,i} + \sum_{j\neq i}\left[\frac{3(\vec{d}_j\cdot\vec{n}_{ji})\cdot\vec{n}_{ji} - \vec{d}_j}{\varepsilon_0\cdot r_{ij}^3}(1 - ik\sqrt{\varepsilon_0}r_{ij}) + k^2\frac{\vec{d}_j - (\vec{d}_j\cdot\vec{n}_{ji})\cdot\vec{n}_{ji}}{r_{ij}}\right]e^{ik\sqrt{\varepsilon_0}r_{ij}}\right) \quad (7)$$

In the matrix form, we can write $\vec{d} = \hat{\alpha}\cdot\vec{E}_{\mathrm{ext},\omega} + \hat{\beta}\cdot\vec{d}$, where the dipole vector is defined as $\vec{d} = (d_{1,x}, d_{1,y}, d_{1,z}, d_{2,x}, d_{2,y}, d_{2,z},\ldots)$ and the electric field vector $\vec{E}_{\mathrm{ext},\omega,i}$ is defined in a similar way. The formal solution of the matrix equation is obvious: $\vec{d}_i = \hat{T}\cdot\vec{E}_{ext,\omega}$, where $\hat{T} = (1 - \hat{\beta})^{-1}\hat{\alpha}$. For the components, $d_{i,\gamma} = E_0\sum_{j,\gamma'=x,y,z}T_{ij,\gamma\gamma'}\cdot e_{0,\gamma'}e^{i\vec{k}\vec{r}_j}$. However, the final results will be obtained numerically for $N_{\mathrm{NP}} > 2$, where N_{NP} is the number of NPs in a complex.

CD for Complexes of Small Size. First we derive an equation for CD in NP complexes with small sizes in which internal retardation effects are weak. In the next section, we will check numerically how strong the internal retardation effects are. Since the internal retardation effects are neglected, eq 5 is valid. We now expand the external field: $\vec{E}_{\mathrm{ext},\omega,i} = \vec{e}_0E_0e^{i\vec{k}\vec{r}} \approx \vec{e}_0E_0(1 + i\vec{k}\vec{r})$. The CD signal appears due to the second term in this expansion and comes from the retardation effect in the incident wave, $\varepsilon_{CD} \propto (kR)\cdot\varepsilon_\pm \propto (R/\lambda_0)\cdot\varepsilon_\pm$.[1] Here, R is a size of a complex. In the Supporting Information, we give a few more details of the derivation. The CD signal in the dipole limit takes the form

$$\varepsilon_{CD,1} = -\left(\frac{N_A}{0.23}\right)10^4\varepsilon_0\frac{8\pi}{2\cdot c_0\sqrt{\varepsilon_0}}\omega\cdot\frac{k}{3}\mathrm{Im}\left[\left(\sum_{i,j}(T_{ij,xy} - T_{ij,yx})r_{ij,z} + (T_{ij,yz} - T_{ij,zy})r_{ij,x} + (T_{ij,zx} - T_{ij,xz})r_{ij,y}\right)\right] \quad (8)$$

In eq 8, we can see explicitly that the CD effect originates from the absence of mirror symmetries in the complex. In the quantum theory, the CD strength is given by $CD_{\mathrm{quantum}} \propto \mathrm{Im}[\vec{\mu}_{12}\cdot\vec{m}_{21}]\cdot\rho_{DOS}$[1], where $\vec{\mu}_{12}$ and $\vec{m}_{21}$ are the quantum-mechanical matrix elements of the operators of electric and magnetic moments, respectively, and ρ_{DOS} is the density of excited states of a quantum object (e.g., a molecule). In fact, eq 8 is the classical version for the quantum-mechanical quantity $\mathrm{Im}[\vec{\mu}_{12}\cdot\vec{m}_{21}]\cdot\rho_{\mathrm{DOS}}$.

General Properties of the CD Spectrum. In the next section, we will numerically calculate the CD signals from few NP complexes using eq 6. For our relatively small complexes (~10 nm), the internal retardation effects are not strong; these effects are included in eq 3 since this equation involves the photon wavevector k. Nevertheless, we will estimate numerically these effects. Since we are using the dipole approximation, the inter-NP distances should be

DOI: 10.1021/nl101231b | Nano Lett. 2010, 10, 2580–2587

taken relatively large, $r_{ij} > 3 \cdot (a_i + a_j)/2$.[16,19] For our complex with $r_{ij} \sim 15$ nm and $a_i \sim 5$ nm, the inter-NP interactions are relatively weak and the dipole approximation is applied. We can estimate the NP−NP interactions by looking at the ratio between the Coulomb-induced electric field and the incident electric field and we found that $|\vec{E}_{\text{induced},\omega,i}|/|\vec{E}_{\text{external},\omega,i}| < 0.1$.

It is essential to look at the expansions of optical cross sections in term of k, assuming $kR = 2\pi R/\lambda_0 \ll 1$, where R is a size of a complex. The absorption cross sections of a small NP complex are $\sigma_+ \approx \sigma_- \propto k \cdot R^3$. Then, the light scattering cross section is $\sigma_{\text{scat}} \propto k^4 \cdot R^6$.[35] Regarding the CD cross section, we can obtain the following important expansion

$$\sigma_{\text{CD}} = \sigma_+ - \sigma_- \approx b_2 \cdot k^2 + b_4 \cdot k^4 + \ldots$$

The first term ($\propto k^2$) is the leading contribution for small complexes ($kR \ll 1$). When a complex is tightly packed with NPs (NP−NP surface-to-surface separations are smaller than the NP radii) and NP−NP interactions are very strong, we obtain from a simple dimensionality analysis, $b_2 \propto R^4$. Even in a tightly packed chiral complex with strong NP−NP interactions, the CD signal ($\sigma_{CD} \propto k^2R^4$) can be essentially weaker than the absorption $\sigma_0 = (\sigma_+ + \sigma_-)/2 \propto kR^3$ because the CD signal comes from the retardation effects and, therefore, includes an additional small parameter $k \cdot R$. In reality, the CD signal is even weaker than $kR \cdot \sigma_0$, since the CD effect requires an object to be of low symmetry (chiral) and additional small numerical factors appear. Here we mostly consider relatively diluted complexes with relatively weak NP−NP interactions. For identical NPs ($a_i = a_0$) and a relatively diluted complex ($r_{ij} > 3 \cdot a_0/2$), we apply the dipole approximation and obtained numerically the following result:

$$b_2 = \eta(\omega)\frac{a^{12}}{R^8} \tag{9}$$

where the dimensionless function $\eta(\omega)$ depends on the dielectric constant of NPs and contains the plasmon resonances.

In our calculations, we will see that the plasmonic CD spectrum has both positive and negative bands. The reason is that the NP−NP Coulomb coupling in a chiral NP assembly splits plasmon resonances of individual NPs and creates preferentially left-handed collective plasmonic modes on one side of the plasmon resonance and right-handed modes on the other side. We can see similar positive and negative bands in the CD spectra of many biomolecular systems such as the α-helix[1,33,36] where the CD signal comes from the dipole−dipole interaction between residues (chromophores).

Numerical Results. *Helix.* We now consider a set of NP complexes that resemble biomolecules with helical or coil structures. We assume Au-NPs and a bulk dielectric constant of the metal.[37] The optical dielectric constant of matrix $\varepsilon_0 = 1.8$ (water). The numbers of NPs in a helix will be $N_{\text{NP}} = 4$, 5, 6, and 7; the complexes with $N_{\text{NP}} = 1-3$ do not show a CD signal since they have mirror symmetry planes. The positions of NPs in the helix are given by $x_i = R_0 \cos[i \cdot \varphi_0]$, $y_i = R_0 \sin[i \cdot \varphi_0]$, and $z_i = \text{step} \cdot i \cdot \varphi_0/(2\pi)$, where $i = 1, 2, \ldots N_{\text{NP}}$. The geometrical parameters are chosen in the following way: $a_i = 5$ nm, $R_0 = 12$ nm, $\varphi_0 = \pi/2$, and step = 15 nm. Inserts in Figure 3 show such complexes. We start with the simplest complex $N_{\text{NP}} = 4$ that exhibits nonzero CD effect (Figure 2). One can see that the CD strength is much less than the extinction $\varepsilon_{\text{CD}}/\varepsilon \sim 10^{-5}$. This is typical for the CD effect. This is because the dipole−dipole interactions are relatively weak for our complex and the CD strength has an additional small parameter kR. In fact, the influence of the NP−NP coupling on the extinction is less than 1%.

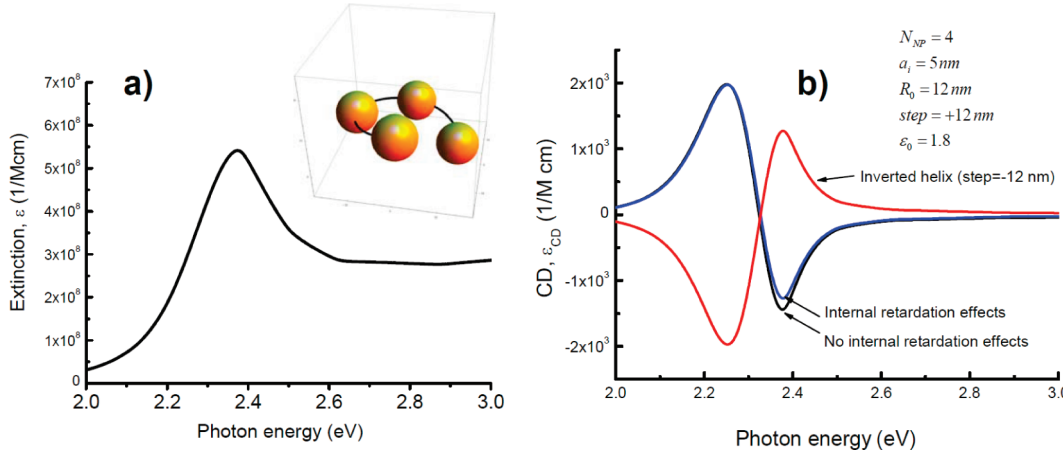

FIGURE 2. (a) Extinction of the helical complex with $N_{\text{NP}} = 4$. Insert shows the model. (b) Calculated CD spectra for the helix with $N_{\text{NP}} = 4$ and its mirror image. Also, the graph shows the internal retardation effect in the complex is small.

DOI: 10.1021/nl101231b | *Nano Lett.* **2010,** *10,* 2580–2587

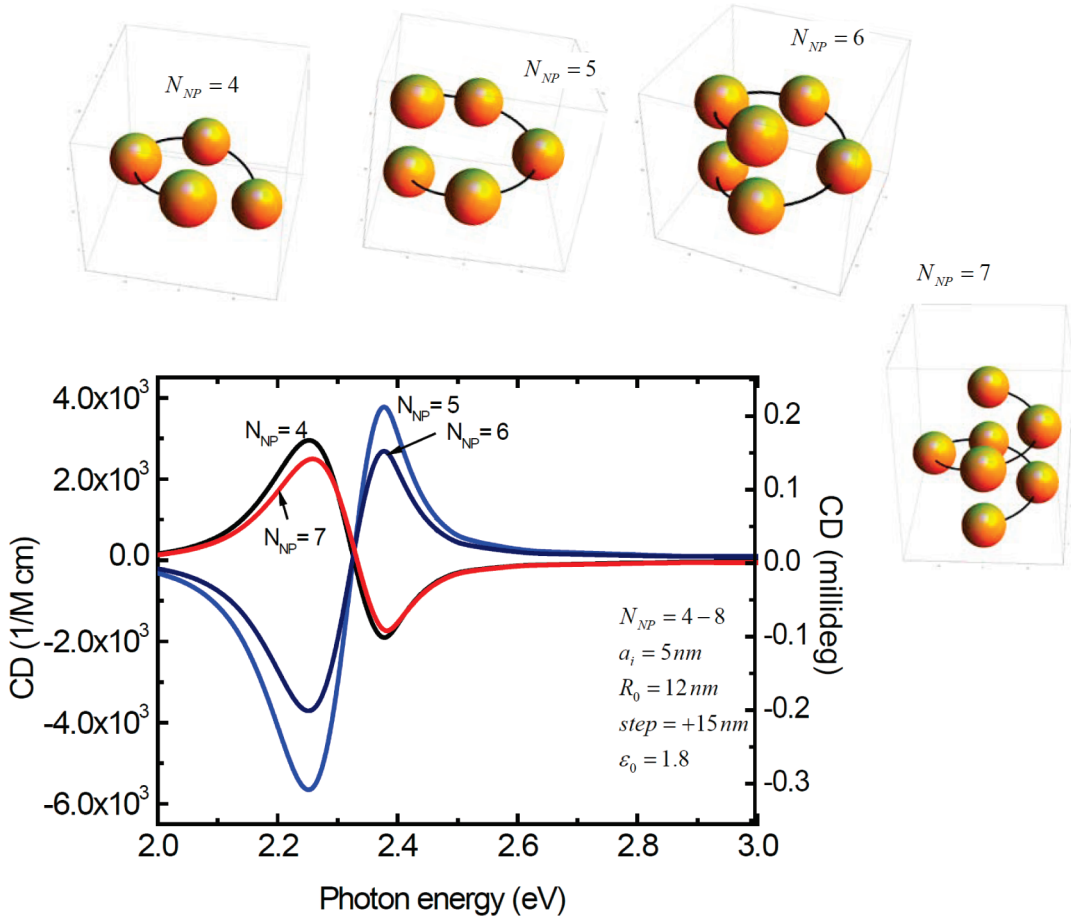

FIGURE 3. Calculated CD spectra of helix complexes (N_{NP} = 4, 5, 6, and 7) with the parameters given in the text. Inserts: models of the complexes.

Another observation from Figure 2 is that the internal retardation effects are weak and do not change essentially the CD line shape. Such helical NP complexes can be assembled using DNA and peptide nanostructures as templates.[20,23]

Figure 3 presents results for helices with N_{NP} = 4, 5, 6, and 7. We can see that the number of NPs in a helix is very important and the CD line shape can change dramatically with increase of N_{NP}. In particular, when we move from N_{NP} = 4 to N_{NP} = 5, the CD spectrum becomes flipped and also enhanced. This strong change in the CD spectrum occurs because the CD signal comes from NP−NP interactions and is very sensitive to the geometry of a complex. For large complexes, the internal retardation effects become more important and this case should be investigated specially including the light scattering contribution. Here we limit ourselves to relatively small complexes $N_{NP} \leq 7$ in which the internal retardation effect is a small correction to the CD rate (less than 5% for the peak values).

In Figure 3, we also give the CD strength in the units of millidegrees, which are often used in the experimental graphs. The CD strength in the units of degrees[1] is obtained as $\theta(\text{deg}) = 32.98 \cdot \Delta A = 32.98 \cdot C \cdot l_{opt} \cdot \varepsilon_{CD}$, where C and l_{opt} are the molar concentration of complexes (in M) and optical path (in cm), respectively. Then, ε_{CD} should be taken in the usual units ($M^{-1} \cdot cm^{-1}$). For estimations in Figure 3, we took the following typical numbers l_{opt} = 1 cm and $C = 1.7 \times 10^{-9}$ M that give the peak absorbance $A = C \cdot l_{opt} \cdot \varepsilon \sim 1$ for our complexes with N_{NP} = 4−7.

Tetramer. Au-NP tetramer can be assembled on a cubic nanocrystal made of DNA or another material (Figure 4a). Again we see that the CD signal is really sensitive to the geometry. Two tetramers with overall similar parameters have inverted CD spectra (Figure 4c). Typically we observe in our calculations that chiral complexes with symmetric frames give weaker CD signals. In this case, two complexes (with symmetric and asymmetric frames) give similar CD signals since the tetramer 2 (symmetric frame) has two NPs (nos. 3 and 4) which have relatively small surface-to-surface distance; this factor enhances the CD signal for the tetramer 2.

We note that, in our definition, a "frame" is a set of points that are the positions of NP centers. A chiral complex may have a symmetric frame if NPs involved in this complex have different radii; one example is shown in Fig. 4b (tetramer 2 having a symmetric frame with the mirror x-z plane). A complex with a symmetric frame and all identical NPs is, of course, non-chiral.

DOI: 10.1021/nl101231b | *Nano Lett.* **2010,** *10,* 2580–2587

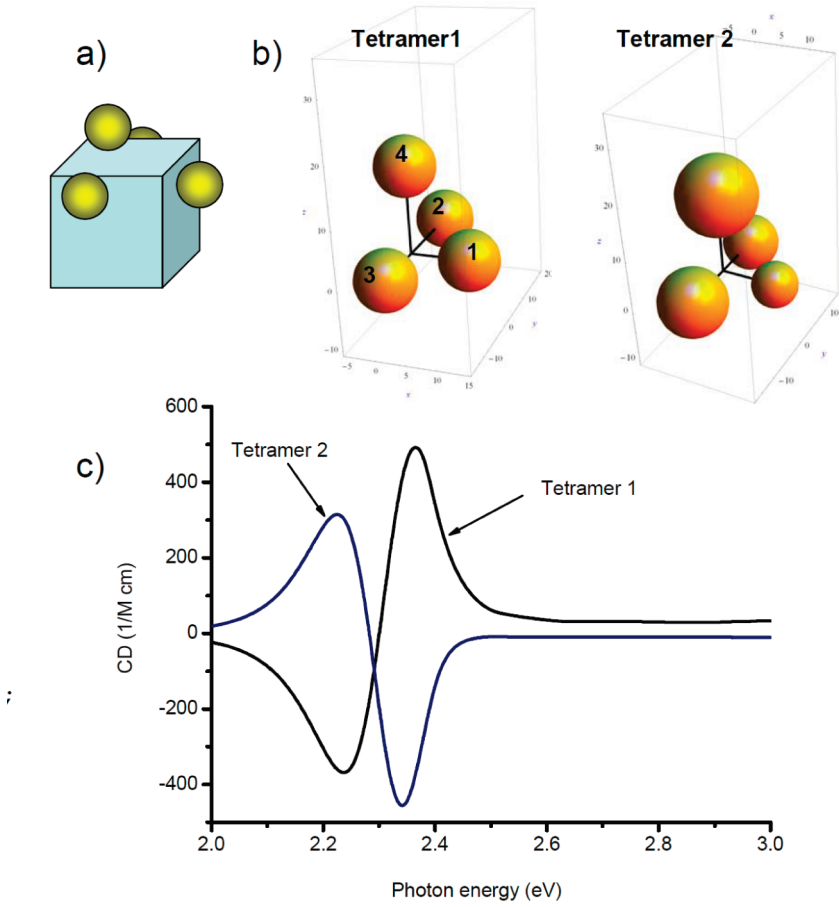

FIGURE 4. (a,b) Models of the complexes with the tetramer frame. (c) Calculated CD spectra of the complexes shown in (b). The geometry of the complex is defined by the following parameters: $r_1 = (a,0,0)$, $r_2 = (0,1.5a,0)$, $r_3 = (0,-a,0)$, $r_4 = (0,0,1.5a)$, $a_i = 5$ nm, $a = 10$ nm (tetramer 1, asymmetric frame) and $r_1 = (a,0,0)$, $r_2 = (0,a,0)$, $r_3 = (0,-a,0)$, $r_4 = (0,0,1.5a)$, $a_1 = 4$ nm, $a_2 = 5$ nm, $a_3 = 6$ nm, $a_4 = 7$ nm, $a = 10$ nm (tetramer 2, symmetric frame).

Pyramids. The pyramidal complexes and their CD spectra are shown in Figure 5. Here we can see two important effects. For two asymmetric frames with identical NPs, the CD strength decreases very rapidly with decreasing of the size of NP ($\propto a^{1.2}$); the reason is that the CD comes from the Coulomb interaction between NPs and NP−NP interactions weaken with decreasing a size of NPs. The second effect is that a chiral complex with a symmetric frame has rather small CD signal. Within the dipole approach, we observe this effect on many complexes.

Tetrahedron. A complex with the tetrahedral frame is chiral if all four NPs at the vertices are different. Using the dipole approximation, we found numerically that the coefficient b_2 in the leading term of the CD effect of a chiral tetrahedral complex is vanishing. Our conclusion is that a tetrahedral NP complex in the dipole approximation has a very weak CD signal. The reason is that the frame is highly symmetric, having six mirror planes. It can be that multipole interactions can lead to a nonvanishing coefficient b_2 in this complex. In the case of a pyramidal frame (see above), we also found that a chiral complex with a symmetric pyramidal frame (one symmetry plane for the frame; see upper part of Figure 5) has a weak CD. Our general conclusion is that chiral complexes with symmetric frames may have weaker CD signals within the dipole model.

Discussion and Conclusions. Since the CD response in our complexes comes from Coulomb interactions between NPs, the CD spectrum is very sensitive to the geometry and composition. In addition, the CD spectrum has typically both positive and negative bands. Therefore, a small variation of geometry or composition of complexes in a macroscopic ensemble in a solution can greatly diminish the CD signal. For example, helical NP complexes with $N_{NP} = 4$ and $N_{NP} = 5$ show inverted CD spectra (Figure 3). If a solution includes both complexes simultaneously (with $N_{NP} = 4$ and $N_{NP} = 5$), the resultant CD can be small. Also, in the best case, a solution should contain complexes of the same chirality, that is, enantiomers of one kind. Or, at least concentrations of opposite enantiomers should be unequal. It is very interesting to compare the plasmonic CD in our complexes and the CD effect in biomolecules. For this, we now introduce a new parameter, volume CD efficiency

DOI: 10.1021/nl101231b | *Nano Lett.* **2010,** *10,* 2580–2587

$$\varepsilon_{CD,V} = \varepsilon_{CD}/V_{complex}$$

This parameter shows a CD signal related to a volume of a chiral object. Keeping in mind potential applications of chiral complexes, one should aim for complexes with a maximized $\varepsilon_{CD,V}$. Then, a film composed of chiral complexes will have maximized chiral properties. In our helical complexes, $|\varepsilon_{CD,V}| \sim 0.6\ cm^{-1} \cdot M^{-1} \cdot nm^{-3}$ for the peak values of the CD spectrum at $\lambda \sim 540$ nm (Figure 2). For the DNA molecules, we can estimate $|\varepsilon_{CD,V}| \sim 9\ cm^{-1} \cdot M^{-1} \cdot nm^{-3}$ at $\lambda \sim 250$ nm; for this estimate, we took the data from refs 38 and 39. We can see that the CD efficiency of NP complexes is somewhat less than that of DNA. However, the CD wavelength becomes strongly increased from 250 to 540 nm. Of course, the molar CD signals in Au-NP complexes can be much stronger than those in DNA, $\varepsilon_{CD,Au-complex,max} \sim 6 \times 10^3\ cm^{-1} \cdot M^{-1}$ and $\varepsilon_{CD,DNA,max} \sim 15\ cm^{-1} \cdot M^{-1}$. The molar CD strength for DNA is calculated in terms of the molarity of small nucleotide units, while the molar CD signal of Au-system is given for the molarity of relatively large NP complexes. Another convenient parameter to compare the properties of artificial NP complexes and biomolecules is a chiral-anisotropy factor

$$\varepsilon_{CD,\varepsilon} = \varepsilon_{CD}/\varepsilon_{complex}$$

For the helical Au-NP complex, $\varepsilon_{CD,\varepsilon} \sim 10^{-5}$, whereas for DNA $\varepsilon_{CD,\varepsilon} \sim 10^{-3}$. We see that the NP complexes with the chosen parameters cannot compete yet with the helical biomolecules that comprise tightly packed and strongly interacting chromophores. We note that the CD effect in NP complexes can be strongly enhanced, compared with the

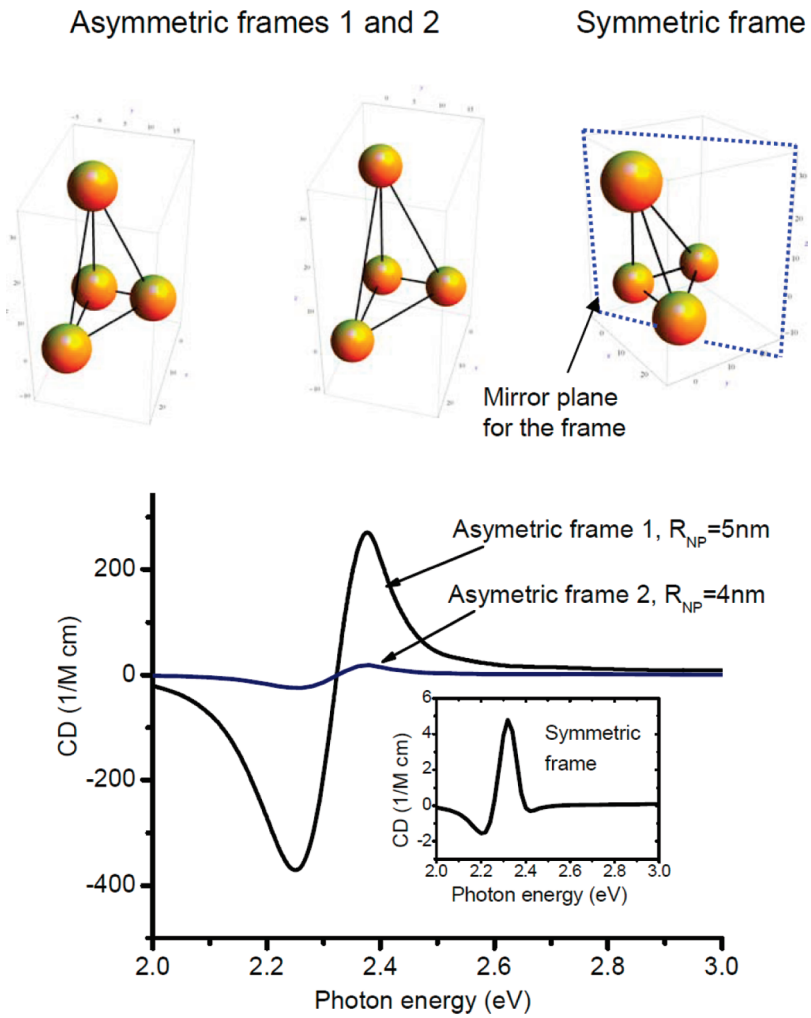

FIGURE 5. (Upper part) Models of chiral NP pyramids. (Lower part) Calculated CD spectra of pyramidal complexes with asymmetric frames. (Insert) Calculated CD for the complex with a symmetric frame. The geometries of the complexes in this figure are defined by the following positions and parameters: $r_1 = (0,0,0)$, $r_2 = (0,0,2a)$, $r_3 = (1.5a,0,0)$, $r_4 = (0,a,0)$, $a_i = 5$ nm, $a = 13$ nm (asymmetric frame 1) and $r_1 = (0,0,0)$, $r_2 = (0,0,2a)$, $r_3 = (1.5a,0,0)$, $r_4 = (0,a,0)$, $a_i = 4$ nm, $a = 13$ nm (asymmetric frame 2) and $r_1 = (0,0,0)$, $r_2 = (0,0,2a)$, $r_3 = (1.5a,0,0)$, $r_4 = (0,1.5a,0)$, $a_1 = 5$ nm, $a_2 = 7$ nm, $a_3 = 6$ nm, $a_4 = 5$ nm, $a = 13$ nm (symmetric frame).

DOI: 10.1021/nl101231b | *Nano Lett.* **2010,** *10,* 2580–2587

values calculated here, by reducing the NP−NP distances. However, to simulate complexes with smaller NP−NP distances, one should employ the multipole expansion.[12] We also note that this paper describes a particular class of "discrete" nanostructures composed of single NPs. More possibilities to create a strong plasmonic CD effect can appear in continuous chiral nanostructures with strong plasmon resonances.

To conclude, NP complexes with plasmon resonances offer the possibility to create strong optical chirality in the visible region. The geometry and composition of NP complexes are crucial. In our numerical calculations, we found that helical complexes, which resemble biomolecules, have stronger CD signals compared to pyramidal assemblies. As a final remark, we note that the predicted CD mechanism can also be realized using exciton resonances in semiconductor NPs.

Acknowledgment. This work was supported by NSF (project number CBET-0933415), Air Force Research Laboratories, Dayton, Ohio, and BNNT Initiative at Ohio University.

Supporting Information Available. Derivation of the CD extinction in the dipole limit. This material is available free of charge via the Internet at http://pubs.acs.org.

REFERENCES AND NOTES

(1) *Circular dichroism and the conformational analysis of biomolecules*; Fasman, G. D., Ed.; Plenum: New York, 1996.
(2) Pendry, J. B. *Science* **2004**, *306*, 1353–1355.
(3) Bruchez, Jr, M.; Moronne, M.; Gin, P.; Weiss, S.; Alivisatos, A. P. *Science* **1998**, *281*, 2013.
(4) Chan, W. C. W.; Nie, S. *Science* **1998**, *281*, 2016.
(5) Prodan, E.; Radloff, C.; Halas, N. J.; Nordlander, P. *Science* **2003**, *302*, 419–422.
(6) Crookes-Goodson, W. J.; Slocik, J. M.; Naik, R. R. *Chem. Soc. Rev.* **2008**, *37*, 2403–2412.
(7) Grote, J. G. *J. Nanophotonics* **2008**, *2*, No. 020301.
(8) Tang, Y.; Ouyang, M. *Nat. Mater.* **2007**, *6*, 754–759.
(9) Dulkeith, E.; Ringler, M.; Klar, T. A.; Feldmann, J.; Munoz Javier, A.; Parak, W. J. *Nano Lett.* **2005**, *5*, 585.
(10) Fofang, N. T.; Park, T. H.; Neumann, O.; Mirin, N. A.; Nordlander, P.; Halas, N. J. *Nano Lett.* **2008**, *8*, 3481–3487.
(11) Lee, J.; Govorov, A. O.; Dulka, J.; Kotov, N. A. *Nano Lett.* **2004**, *4*, 2323.
(12) Govorov, A. O.; Bryant, G. W.; Zhang, W.; Skeini, T.; Lee, J.; Kotov, N. A.; Slocik, J. M.; Naik, R. R. *Nano Lett.* **2006**, *6*, 984.
(13) (a) Rogach, A. L.; Klar, T. A.; Lupton, J. M.; Meijerinkd, A.; Feldmann, J. *J. Mater. Chem* **2009**, *19*, 1208. (b) Kaniber, S. M.; Simmel, F. C.; Holleitner, A. W.; Carmeli, I. *Nanotechnology* **2009**, *20*, 345701. (c) Govorov, A. O.; Carmeli, I. *Nano Lett.* **2007**, *7*, 620–625. (d) Govorov, A. O. *Adv. Mater.* **2008**, *20*, 4330–4335.
(14) Wei, H.; Ratchford, D.; Li, X. Q.; Xu, H. X.; Shih, C. K. *Nano Lett.* **2009**, *9*, 4168–4171.
(15) (a) Citrin, D. S. *Opt. Lett.* **1995**, *20*, 901–903. (b) Citrin, D. S. *Nano Lett.* **2005**, *5*, 5985–989.
(16) Maier, S. A.; Kik, P. G.; Atwater, H. A. *Phys. Rev. B* **2003**, *67*, 205402.
(17) Schuller, J. A.; Barnard, E. S.; Cai, W. S.; Jun, Y. C.; White, J. S.; Brongersma, M. L. *Nat. Mater.* **2010**, *9*, 193–204.
(18) (a) Brandl, D. W.; Mirin, N. A.; Nordlander, P. *J. Phys. Chem. B* **2006**, *110*, 12302–12310. (b) Gomez, D. E.; Vernon, K. C.; Davis, T. J. *Phys. Rev. B* **2010**, *81*, 075414.
(19) (a) Weber, W. H.; Ford, G. W. *Phys. Rev. B* **2004**, *70*, 125429. (b) Zhen, Y.-R.; Fung, K. H.; Chan, C. T. *Phys. Rev. B* **2008**, *78*, 035419.
(20) Chen, C. L.; Zhang, P. J.; Rosi, N. L. *J. Am. Chem. Soc.* **2008**, *130*, 13555.
(21) Chen, W.; Bian, A.; Agarwal, A.; Liu, L.; Shen, H.; Wang, L.; Xu, C.; Kotov, N. A. *Nano Lett.* **2009**, *9*, 2153–2159.
(22) Mastroianni, A. J.; Claridge, S. A.; Alivisatos, A. P. *J. Am. Chem. Soc.* **2009**, *131*, 8455–8459.
(23) Douglas, S. M.; Dietz, H.; Liedl, T.; Högberg, B.; Graf, F.; Shih, W. M. *Nature* **2009**, *459*, 414–418.
(24) (a) Schaaff, T. G.; Whetten, R. L. *J. Phys. Chem. B* **2000**, *104*, 2630–2641. (b) Roman-Velazquez, C. E.; Noguez, C.; Garzon, I. L. *J. Phys. Chem. B* **2003**, *107*, 12035. (c) Li, T. H.; Park, H. G.; Lee, H. S.; Choi, S. H. *Nanotechnology* **2004**, *15*, S660–S663. (d) Gautier, C.; Bürgi, T. *J. Am. Chem. Soc.* **2006**, *128*, 11079–11087. (e) Shemer, G.; Krichevski, O.; Markovich, G.; Molotsky, T.; Lubitz, I.; Kotlyar, A. B. *J. Am. Chem. Soc.* **2006**, *128*, 11006–11007.
(25) Nakashima, T.; Kobayashi, Y.; Kawai, T. *J. Am. Chem. Soc.* **2009**, *131*, 10342.
(26) Elliott, S. D.; Moloney, M. P.; Gun'ko, Y. K. *Nano Lett.* **2008**, *8*, 2452–2457.
(27) Ha, J.-M.; Solovyov, A.; Katz, A. *Langmuir* **2009**, *25*, 153–158.
(28) Kitaev, V. *J. Mater. Chem.* **2008**, *18*, 4745–4749.
(29) Lieberman, I.; Shemer, G.; Fried, T.; Kosower, E. M.; Markovich, G. *Angew. Chem., Int. Ed.* **2008**, *47*, 4855.
(30) Govorov, A. O.; Fan, Z.; Hernandez, P.; Slocik, J. M.; Naik, R. R. *Nano Lett.* **2010**, *10*, 1374–1382.
(31) Drachev, V. P.; Bragg, W. D.; Podolskiy, V. A.; Safonov, V. P.; Kim, W. T.; Ying, Z. C.; Armstrong, R. L.; Shalaev, V. M. *J. Opt. Soc. Am. B* **2001**, *18*, 1896.
(32) Kuwata-Gonokami, M.; Saito, N.; Ino, Y.; Kauranen, M.; Jefimovs, K.; Vallius, T.; Turunen, J.; Svirko, Y. *Phys. Rev. Lett.* **2005**, *95*, 227401.
(33) *Circular Dichroism: Principles and Applications*, 2nd ed.; Berova, N., Nakanishi, K., Woody, R. W., Eds.; Wiley-VCH: New York, 2000.
(34) Jackson, J. D. *Classical Electrodynamics*, 3rd ed.; Wiley: New York, 1998.
(35) van de Hulst, H. C. *Light Scattering by Small Particles*; Dover: New York, 1981.
(36) Woody, W. W. In *Circular dichroism and the conformational analysis of biomolecules*; Fasman, G. D., Ed.; Plenum: New York, 1996; pp. 25−67.
(37) Johnson, P. B.; Christy, R. W. *Phys. Rev. B.* **1972**, *6*, 4370–4379.
(38) Kypr, J.; Vorlickova, M. *Biopolymers* **2002**, *67*, 275–277.
(39) Ren, J.; Chaires, J. B. *Biochemistry* **1999**, *38*, 16067–16075.

DOI: 10.1021/nl101231b | *Nano Lett.* **2010,** *10,* 2580--2587